Two-pion exchange as a leading-order contribution in chiral effective field theory

Chinmay Mishra,[1] A. Ekström,[2] G. Hagen,[3,1] T. Papenbrock,[1,3] and L. Platter[1,3,4]
[1]*Department of Physics and Astronomy, University of Tennessee, Knoxville, Tennessee 37996, USA*
[2]*Department of Physics, Chalmers University of Technology, SE-412 96 Göteborg, Sweden*
[3]*Physics Division, Oak Ridge National Laboratory, Oak Ridge, Tennessee 37831, USA*
[4]*Institut für Kernphysik, Technische Universität Darmstadt, 64289 Darmstadt, Germany*

(Received 1 December 2021; revised 1 April 2022; accepted 12 August 2022; published 25 August 2022)

Pion exchange is the central ingredient to nucleon-nucleon interactions used in nuclear structure calculations, and one-pion exchange (OPE) enters at leading order in chiral effective field theory. In the $^{2S+1}L_J = {}^1S_0$ partial wave, however, OPE and a contact term needed for proper renormalization fail to produce the qualitative, and quantitative, features of the scattering phase shifts. Cutoff variation also revealed a surprisingly low breakdown momentum $\Lambda_b \approx 330$ MeV in this partial wave. Here we show that potentials consisting of OPE, two-pion exchange (TPE), and a single contact address these problems and yield accurate and renormalization group (RG) invariant phase shifts in the ${}^1S_0$ partial wave. We demonstrate that a leading-order potential with TPE can be systematically improved by adding a contact quadratic in momenta. For momentum cutoffs $\Lambda \lesssim 500$ MeV, the removal of relevant physics from TPE loops needs to be compensated by additional contacts to keep RG invariance. Inclusion of the Δ isobar degree of freedom in the potential does not change the strong contributions of TPE.

DOI: 10.1103/PhysRevC.106.024004

I. INTRODUCTION

Ever since its introduction by Yukawa [1], boson exchange has been central to the theory of nuclear interactions. In quantum chromodynamics, chiral symmetry is spontaneously and explicitly broken, and the pion emerges as the corresponding pseudo-Nambu-Goldstone boson. Pion exchange, together with contact interactions that account for unknown short-range physics, thus are the ingredients in a chiral effective field theory (EFT) description of the nucleon-nucleon interaction [2–9].

In chiral EFT, and within the commonly employed Weinberg power counting, the leading-order contributions to the nucleon-nucleon interaction consist of one-pion exchange (OPE) and one contact each in the ${}^1S_0$ and ${}^3S_1$ partial waves. At next-to-leading order (NLO) in Weinberg counting the leading two-pion exchange (TPE) contributions as well as contacts quadratic in momenta enter.

Statistical analyses of higher-order chiral EFT predictions for nucleon-nucleon scattering data infer a breakdown momentum $\Lambda_b \approx 600$–700 MeV, and that higher chiral orders yield systematical improvements in powers of $Q/\min(\Lambda, \Lambda_b)$ beyond the leading-order results in the Weinberg power counting [10–12]. Here Q is the low-momentum scale of interest, e.g., the external momentum in nucleon-nucleon scattering, and Λ is the cutoff employed in the regularization of the theory. While this looks encouraging, there are well-known challenges [13], and we mention two of them.

First, recent computations in the Weinberg [14] and a modified power counting [15] show that leading-order chiral EFT potentials predict light-mass nuclei that are unstable with respect to breakup into α particles and lighter-mass clusters, raising questions about what should be expected from a nuclear EFT at leading order. Of course, the lack of any spin-orbit contributions at leading order in the Weinberg power counting would also presumably make well-known nuclear shell structure a subleading effect.

Second, the leading-order description of nucleon-nucleon phase shifts in the ${}^1S_0$ partial wave are problematic in the Weinberg power counting [15–31] (see Ref. [32] for a recent review). The combination of OPE and a single contact fails qualitatively to capture the pronounced peak at 60°–70° in the phase shift at about 8 MeV of laboratory scattering energy (see blue dotted line in Fig. 1). For all results in this figure, the ${}^1S_0$ contact is adjusted to the reference phase shifts of the potential [33] (shown as a solid black line) at a laboratory scattering energy $E = 15$ MeV. This energy matches the relevant scale of pion physics as $m_\pi^2/m_N \approx 20$ MeV using the pion and nucleon masses m_π and m_N, respectively. The OPE phase shifts are much too attractive beyond the matching point and clearly fail to capture the characteristics of the reference phase shifts. Also, the slope of the OPE phase shift has the wrong sign. We note that the interaction consisting of OPE plus subleading TPE is more accurate than OPE plus leading TPE. This is an indication that the role of subleading TPE might not be correctly reflected in the Weinberg power counting.

Another problem concerns the breakdown momentum Λ_b. The analysis of the ${}^1S_0$ phase shifts by Lepage [34] showed that a potential consisting of OPE plus leading and subleading contacts leads to $\Lambda_b \approx 330$ MeV in the ${}^1S_0$ partial wave. Later

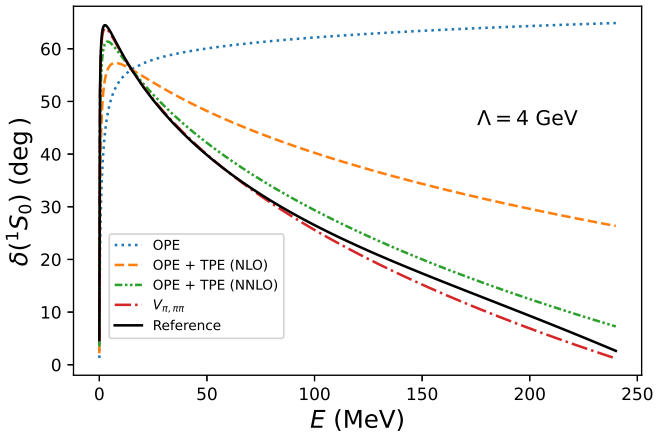

FIG. 1. Nucleon-nucleon phase shifts in the $^1S_0$ partial wave versus the laboratory scattering energy E for various chiral interactions. The momentum cutoff is set to 4 GeV and in all cases a single contact $V_{\rm ct}^{(0)}$ is adjusted to match the phase shift to that of the reference potential (high-precision Idaho-N3LO) by Entem and Machleidt [33] (solid black line) at $E_0 = 15$ MeV. The dotted blue line shows phase shift obtained for OPE, the dashed orange line for OPE plus the leading TPE, the dash-dot-dotted green line for OPE plus subleading TPE, and the dash-dotted red line for the interaction $V_{\pi,\pi\pi}$ consisting of OPE and leading plus subleading TPE (see text for details).

analyses exploring perturbative inclusion of subleading TPE contributions [22,35] confirmed this finding and estimated the breakdown momentum to be even lower, i.e., $\Lambda_{\rm b} \approx 200$ MeV. This questions whether leading-order chiral EFT based on OPE physics is consistent with the general assumption that the breakdown momentum is somewhere between ≈500 and ≈1000 MeV.

Several researchers addressed the shortcoming of too attractive $^1S_0$ phase shifts by adding effective-range corrections [15,36], energy-dependent potentials generated by dibaryon fields [29], or separable potentials [31] to the OPE as leading-order contributions. These approaches improve the phase shifts at a cost of introducing additional parameters. The promotion of TPE to leading order in chiral EFT was proposed already a decade ago by Birse [25] and Pavón Valderrama [37]. We investigate this further; see also the recent papers [38,39].

In this paper we show that chiral physics in the form of TPE, a higher-order correction in the Weinberg power counting, remedies the shortcomings of highly attractive $^1S_0$ phase shifts and without increasing the number of parameters. As Fig. 1 shows, the inclusion of the long-range part of TPE at leading order significantly improves the accuracy of the $^1S_0$ phase shifts. We will also show that the estimated breakdown momentum in this approach is consistent with expectations from chiral EFT. Of course, promoting TPE to leading order raises the question whether to promote also the momentum-dependent counterterms that accompany it in the Weinberg power counting. Here, we will follow the simplest approach by promoting only the long-range part and requiring renormalizability at the level of amplitudes, i.e., the cutoff independence of observables. It is known [40] that one momentum-independent counterterm (boundary condition) is sufficient to renormalize the singular TPE interaction in the $^1S_0$ channel.

Phenomenology connects TPE with the strong midrange attraction of the nucleon-nucleon force [41,42] which is also attributed to the $f_0(500)$ resonance [43] or the σ meson whose width and mass was determined model independently in Ref. [44]. The latter is a central ingredient of relativistic mean-field theories [45–49] and of alternative proposals to chiral EFT which include the effects of the $f_0(500)$ resonance at leading order via the σ meson [50] or the dilaton [51,52], i.e., the Nambu-Goldstone boson of a broken and hidden scale symmetry.

In the Weinberg power counting TPE enters at NLO, but its strongest contributions involving the pion-nucleon coupling constants c_i, with $i = 1, 3, 4$, enter at next-to-next-to-leading order (NNLO). It is known that these subleading TPE contributions are crucial for quantitatively reproducing the $^1S_0$ phase shifts (see, e.g., Refs. [21,53]). We note, however, that the role of TPE is somewhat obscured in chiral potentials. First, an additional contact potential quadratic in momentum also enters in the $^1S_0$ partial wave at NLO in the Weinberg power counting. Second, several popular potentials [33,54–57] employ relatively low momentum cutoffs and thereby truncate some parts of the TPE strength.

This paper is ordered as follows: In Sec. II we give the explicit form of the OPE and TPE potentials, discuss their relative strengths, and show results for phase shifts in the $^1S_0$ partial wave obtained using the proposed leading-order potential where we have promoted TPE. In Sec. III we show that a subleading contact that is quadratic in momenta systematically improves upon these results. In Sec. IV we show that the inclusion of Δ isobar degrees of freedom does not alter our conclusions about promoting TPE to leading order. We end with a summary in Sec. V.

II. CHIRAL OPE AND TPE POTENTIALS

Canonical chiral EFT descriptions of the nuclear interaction employ a power counting for the pion-nucleon potential as done in chiral perturbation theory. The OPE enters at leading order, and subleading contributions are presumably suppressed by powers of $g_A m_\pi/(4\pi f_\pi) \ll 1$, where $g_A \approx 1.28$ is the axial-vector constant, $m_\pi \approx 140$ MeV is the pion mass, and $f_\pi \approx 92$ MeV is the pion-decay constant. The OPE potential is given by

$$V_{\rm OPE}(\mathbf{q}) = -\frac{g_A^2}{4f_\pi^2}\boldsymbol{\tau}_1\cdot\boldsymbol{\tau}_2\frac{(\boldsymbol{\sigma}_1\cdot\mathbf{q})(\boldsymbol{\sigma}_2\cdot\mathbf{q})}{m_\pi^2+q^2}. \tag{1}$$

Here, $\mathbf{q} = \mathbf{p}' - \mathbf{p}$ is the momentum transfer. The Pauli matrices of nucleon j in spin and isospin space are denoted as σ_j and τ_j, respectively. The TPE potentials considered in this work can be written as

$$\begin{aligned} V_{\rm TPE}(\mathbf{q}) = {} & V_C(q) + \boldsymbol{\tau}_1\cdot\boldsymbol{\tau}_2 W_C(q) \\ & + [V_T(q) + \boldsymbol{\tau}_1\cdot\boldsymbol{\tau}_2 W_T(q)](\boldsymbol{\sigma}_1\cdot\mathbf{q})(\boldsymbol{\sigma}_2\cdot\mathbf{q}) \\ & + [V_S(q) + \boldsymbol{\tau}_1\cdot\boldsymbol{\tau}_2 W_S(q)]\boldsymbol{\sigma}_1\cdot\boldsymbol{\sigma}_2. \end{aligned} \tag{2}$$

The leading TPE potential, i.e., the contributions that enter at NLO in the Weinberg power counting, is given by [6,7,53]

$$W_C = -\frac{L(q)}{384\pi^2 f_\pi^4}\Big[4m_\pi^2(5g_A^4 - 4g_A^2 - 1) + q^2(23g_A^4 - 10g_A^2 - 1) + \frac{48g_A^4 m_\pi^4}{w^2}\Big], \qquad (3)$$

$$V_T = -\frac{V_S}{q^2} = -\frac{3g_A^4 L(q)}{64\pi^2 f_\pi^4},$$

while the subleading contributions that enter at NNLO are [6,7,53]

$$V_C = -\frac{3g_A^2}{16\pi f_\pi^4}\big[2m_\pi^2(2c_1 - c_3) - c_3 q^2\big]\tilde{w}^2 A(q),$$

$$W_T = -\frac{W_S}{q^2} = -\frac{g_A^2}{32\pi f_\pi^4} c_4 w^2 A(q). \qquad (4)$$

Here, we used the shorthand

$$w \equiv \sqrt{4m_\pi^2 + q^2},$$

$$L(q) \equiv \frac{w}{q}\log\frac{w+q}{2m_\pi},$$

$$\tilde{w} \equiv \sqrt{2m_\pi^2 + q^2},$$

$$A(q) \equiv \frac{1}{2q}\arctan\frac{q}{2m_\pi}, \qquad (5)$$

with $q \equiv |\mathbf{q}|$, and the pion-nucleon constants c_i are of the order of m_N^{-1} with m_N denoting the nucleon mass m_N. In what follows we use $c_1 = -0.74$ GeV^{-1}, $c_3 = -3.61$ GeV^{-1}, and $c_4 = 2.44$ GeV^{-1} from Ref. [11], obtained from Roy-Steiner relations [58,59]. (Using c_i values from Ref. [53] did not qualitatively change our findings.) We note here that we have neglected any relativistic corrections (proportional to m_N^{-1}) to the TPE at NNLO, omitted any polynomial contributions, and suppressed the dependence of the functions (5) on the spectral function regulator. In what follows, we discuss these points in more detail.

Relativistic corrections are small and contribute $\mathcal{O}(g_A^2 m_\pi/(16m_N))$ to the dominant potential V_C. The NLO potentials (3) also come with a term quadratic in momentum exchange whose strength depends on the renormalization scale [6]; it is usually neglected because a contact quadratic in momenta also enters in the Weinberg power counting at NLO. We neglect this contact here initially because we will focus on the long-range behavior of TPE predicted by chiral EFT. The TPE in the $^1S_0$ partial wave can be renormalized without it. In other words, we choose the contact quadratic in momenta such that it exactly cancels the purely quadratic term in TPE.

The functions L and A in Eqs. (5) are shown as computed using dimensional regularization [6]. When using spectral function regularization [60,61], they also depend on the cutoff $\Lambda_{\rm SFR}$, and expressions (5) are obtained when taking $\Lambda_{\rm SFR} \to \infty$. In this work we use spectral function regularization and set $\Lambda_{\rm SFR} = 700$ MeV, except as indicated otherwise.

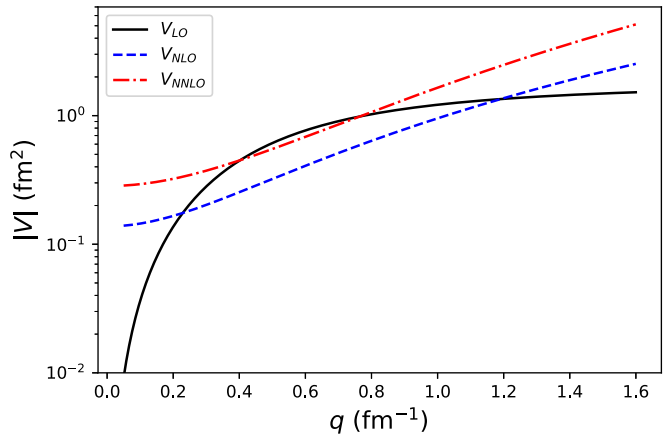

FIG. 2. Long-ranged pion-exchange contributions to the nucleon-nucleon potentials in the spin-singlet/isospin-triplet partial wave at various orders in Weinberg power counting as a function of momentum transfer. The OPE potential (black solid line) is leading order in the Weinberg power counting, the leading TPE (dashed blue line) is NLO, and the subleading TPE (dash-dotted red line) enters at NNLO. Any contributions from terms purely polynomial in momenta are neglected.

We evaluated the long-range pion-exchange potentials in the spin-singlet/isospin-triplet partial waves [where $(\sigma_1 \cdot \mathbf{q})(\sigma_2 \cdot \mathbf{q}) \to -q^2$] and show their magnitudes in Fig. 2 comparing the OPE from Eq. (1), leading TPE from Eqs. (3), and subleading TPE from Eqs. (4) contributions. As expected, OPE is a dominant contribution around $q \approx m_\pi$ while the subleading TPE potential of Eqs. (4) cannot be neglected around momentum transfers of about 1 fm^{-1}. Clearly, at momentum transfers of the order of the pion mass ($m_\pi \approx 0.7$ fm^{-1}) or the Fermi momentum in nuclear matter at saturation ($k_F \approx 1.35$ fm^{-1}), the placement of this TPE potential at NNLO does not reflect its actual strength. Two comments are in order. First, for large momentum transfers $q \gg m_\pi$ we have $V_{LO} \to q^0$, $V_{\rm NLO} \to q^2 \log q$, and $V_{\rm NNLO} \to q^3$. Second, for small momentum transfers $q \to 0$, the OPE indeed scales as q^2 in spin-singlet partial waves.

Let us study the impact of TPE added to OPE in the $^1S_0$ phase shifts. We define a nucleon-nucleon potential in this partial wave that is of the form

$$V(\mathbf{p}', \mathbf{p}) \equiv V_{\pi,\pi\pi} + V_{\rm ct}. \qquad (6)$$

Here, $V_{\pi,\pi\pi}$ consists of OPE and the leading and subleading TPE, while $V_{\rm ct}$ denotes the contact potential to be specified.

At leading order and NLO, the contact potentials are given by

$$V_{\rm ct}^{(0)}(\mathbf{p}', \mathbf{p}) = \tilde{C} \qquad (7)$$

and

$$V_{\rm ct}^{(2)}(\mathbf{p}', \mathbf{p}) = C(p'^2 + p^2), \qquad (8)$$

respectively. The potentials are also regularized via the nonlocal separable regulator

$$V \to f(p'^2/\Lambda^2) V f(p^2/\Lambda^2) \qquad (9)$$

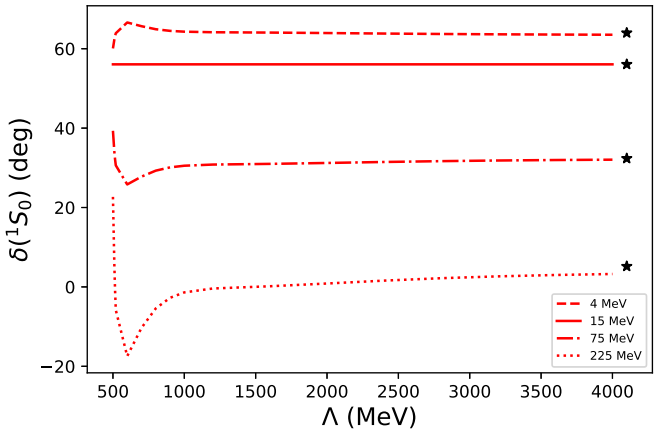

FIG. 3. $^1S_0$ phase shifts as a function of the momentum regulator cutoff Λ at laboratory energies of $E = 4$ (dashed), 15 (solid), 75 (dash dotted), and 225 MeV (dotted) for the potential $V_{\pi,\pi\pi} + V_{\rm ct}^{(0)}$. The black stars show the reference phase shifts at these energies.

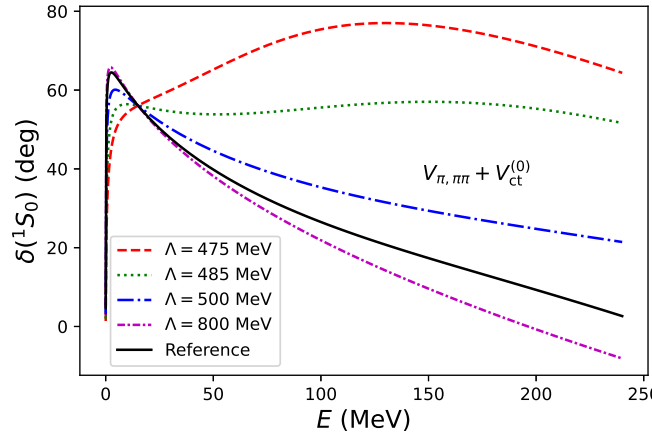

FIG. 4. Phase shifts as a function of laboratory energy of the interaction $V_{\pi,\pi\pi} + V_{\rm ct}^{(0)}$ at low momentum cutoffs as indicated and compared to the reference (solid black line). The phase shifts become increasingly repulsive as the cutoff is increased. For $E > 15$ MeV they cross over and become more repulsive than the reference for cutoffs in the range $500 \lesssim \Lambda \lesssim 520$ MeV.

using $p \equiv |\mathbf{p}|$, $p' \equiv |\mathbf{p}'|$,

$$f(x) = e^{-x^n}, \tag{10}$$

and $n = 3$.

At leading order we adjust the low-energy constant (LEC) $\tilde{C}$ such that the phase shift at the laboratory energy $E_0 = 15$ MeV reproduces the value from the high-precision Idaho-N3LO potential [33], which we take as a reference throughout this work. The precision of this reference is sufficient for our purposes, as the phase shifts of this potential are virtually indistinguishable from a recent partial-wave analysis of nucleon-nucleon scattering data [62].

The $^1S_0$ phase shifts for our leading-order potential are shown as the red dash-dotted line in Fig. 1. For comparison, we also show the results from potentials with other combinations of pion exchanges, such as the sum of OPE and leading TPE (orange dashed line) and OPE plus subleading TPE (green dash-dot-dotted line). The chiral potential $V_{\pi,\pi\pi}$ stands out through its accuracy for scattering energies below and above the energy E_0 used for renormalizing the contact LEC. This suggests that the combination $V_{\pi,\pi\pi}$ of OPE and TPE should be taken as the leading-order contribution from chiral physics in the $^1S_0$ partial wave. This is the main result of this paper. It is consistent with the anticipation obtained from Fig. 2. Although the combination of OPE and leading TPE (shown as the orange dashed line in Fig. 1) brings the phase shift closer to reference, it fails to reproduce the characteristic decrease of the phase shifts with increasing energy, i.e., a lack of increasing repulsion with E, and the amplitude zero is nowhere near $E \approx 250$ MeV. It is also less accurate than the combination of OPE and subleading TPE. This motivates us to promote both the leading and subleading TPE contributions to LO.

We note that the phase shifts presented in Fig. 1 include chiral physics plus a single LEC that accounts for unknown short-range physics. Figure 3 demonstrates that the potential $V_{\pi,\pi\pi} + V_{\rm ct}^{(0)}$ yields renormalization group (RG) invariant $^1S_0$ phase shifts as the cutoff Λ is increased. For a comparison, the reference phase shifts are shown as black stars. Figure 3 also shows that the phase shifts are strongly cutoff dependent for $\Lambda \lesssim 750$ MeV. This can be understood as follows: In coordinate space, the OPE potential exhibits a $1/r^3$ behavior at short distances, where r denotes the two-nucleon relative distance. The TPE potential exhibits a significantly more singular $1/r^6$ short-distance behavior with a typical momentum scale $k_{\pi\pi} \approx 115$ MeV set by the chiral couplings employed in the TPE potential [35]. The cutoff needs therefore to be significantly larger than $k_{\pi\pi}$ to reach convergence. Alternatively, the relevant scale of the TPE interaction can also naively be estimated by

$$\Lambda_{\rm TPE} \equiv \sqrt{2 m_\pi m_N} \approx 510 \text{ MeV}. \tag{11}$$

Cutoffs lower than $\Lambda_{\rm TPE}$ therefore remove physics from the TPE. This effect is highlighted in Fig. 4. As before, we adjusted the leading-order contact $V_{\rm ct}^{(0)}$ to reproduce the reference phase shift at $E_0 = 15$ MeV. We clearly see the effects of removing TPE physics for cutoffs $\Lambda \lesssim 500$ MeV. Indeed, comparison with Fig. 1 shows that the phase shifts at a cutoff of $\Lambda = 475$ MeV are close to those of OPE plus a contact. As we will see below, adding the subleading contact $V_{\rm ct}^{(2)}$ will restore RG invariance in this case.

Figure 4 also allows us to estimate the breakdown momentum in this partial wave as the momentum regulator cutoff value for which the phase shift predictions are closest to the reference [34]. Following this strategy we infer $\Lambda_{\rm b} \approx$ 500–520 MeV. This is significantly larger than what was found when only OPE physics is included at leading order [22,34,35]. It is also in line with expectations from neglecting the physics of more massive exchange mesons.

We repeated the above calculations with cutoffs $\Lambda_{\rm SFR} =$ 900 MeV and 2 GeV in the spectral function regulator. The phase shifts were consistent with RG invariance in these cases as well. Figure 5 demonstrates this for $\Lambda_{\rm SFR} = 2$ GeV. Our

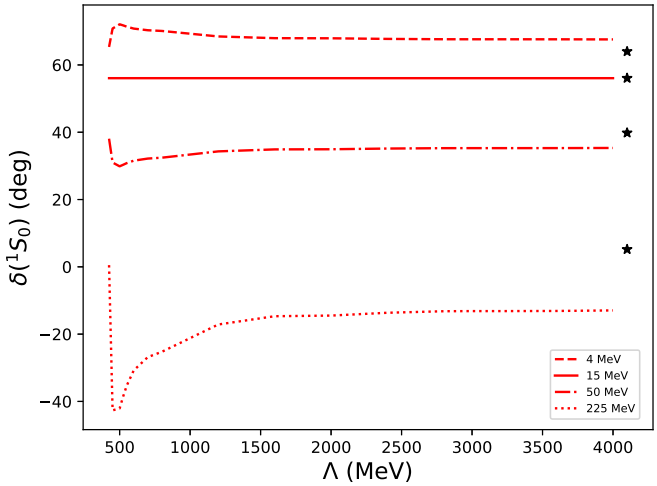

FIG. 5. $^1S_0$ phase shifts as a function of the momentum cutoff Λ using the cutoff $\Lambda_{\rm SFR} = 2$ GeV in the spectral function regularization. Phase shifts are shown at laboratory energies of $E = 4$ (dashed), 15 (solid), 75 (dash dotted), and 225 MeV (dotted) for the potential $V_{\pi,\pi\pi} + V_{\rm ct}^{(0)}$. The black stars show the reference phase shifts at these energies.

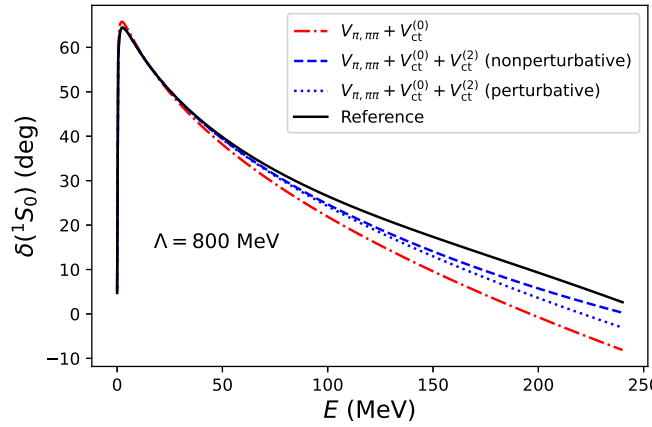

FIG. 6. Systematic improvements of the $^1S_0$ phase shifts by adding the subleading contact $V_{\rm ct}^{(2)}$ to the potential $V_{\pi,\pi\pi} + V_{\rm ct}^{(0)}$. The cutoff is 800 MeV. Results for the potentials $V_{\pi,\pi\pi} + V_{\rm ct}^{(0)}$ and $V_{\pi,\pi\pi} + V_{\rm ct}^{(0)} + V_{\rm ct}^{(2)}$ are shown as a dash-dotted red line and as blue lines, respectively. The dashed and the dotted blue line correspond to the nonperturbative and the perturbative inclusion of the subleading contact $V_{\rm ct}^{(2)}$, respectively, and the solid black line shows the reference.

analysis yields a breakdown scale of about 475 and 425 MeV for $\Lambda_{\rm SFR} = 900$ MeV and 2 GeV, respectively.

III. SYSTEMATIC IMPROVEMENTS

We propose to employ higher-order contacts to systematically improve upon the results of our leading-order potential $V_{\pi,\pi\pi} + V_{\rm ct}^{(0)}$. Thus, contact (8) enters as the subleading correction [34]. This introduces a new LEC, C, and we adjust $\tilde{C}$ and C such that the reference phase shift and its slope are reproduced at the laboratory energy $E_0 = 15$ MeV. In our numerical work, we used the secant slope between E_0 and a second point just below this energy rather than the exact tangent slope. We work at a cutoff of $\Lambda = 800$ MeV.

The question then arises whether one should treat the subleading correction perturbatively, or not. In the nonperturbative approach, the full potential is iterated to solve the Lippmann-Schwinger equation, while the perturbative approach is linear in the subleading correction. We followed both approaches and found similar results for the phase shifts.

Let us discuss the nonperturbative approach. A simultaneous fit of the two LECs $(\tilde{C}, C)$ to the phase shift and its slope at E_0 is somewhat challenging. Instead, we first calibrated $\tilde{C}$ and subsequently determined C such that the reference phase shift is reproduced at E_0. Repeating this procedure for various values of $\tilde{C}$ yields a one-parameter curve $C(\tilde{C})$. Interestingly, we found that this is a quadratic function to very high accuracy. We then moved along this parabola and determined the point where the slope of the phase shift agrees with the reference as well. The resulting phase shifts are shown as a dashed blue line in Fig. 6 and compared to our leading-order results (red dash-dotted line). The improvement is clearly visible. Figure 7 shows the absolute differences between our phase shifts and the reference on a log-log plot. The systematic power-law improvement from the quadratic contact is evident.

We also note that $C\Lambda_{\rm b}^2/\tilde{C} \approx -4$, and this is consistent with EFT expectations, where this dimensionless number should be $\mathcal{O}(1)$ in size.

In a second approach, we treated contact (8) in perturbation theory. Our leading-order theory is adjusted to the reference phase shift at E_0 and the corresponding LECs are $(\tilde{C}, C) = (\tilde{C}_0, 0)$. In a perturbative approach the LECs become $(\tilde{C}_0 + \delta\tilde{C}, \delta C)$ in the presence of the potential $V_{\rm ct}^{(2)}$. We expand the phase shift as

$$\delta(E) \approx \delta(E)|_0 + \left.\frac{\partial\delta(E)}{\partial\tilde{C}}\right|_0 \delta\tilde{C} + \left.\frac{\partial\delta(E)}{\partial C}\right|_0 \delta C. \qquad (12)$$

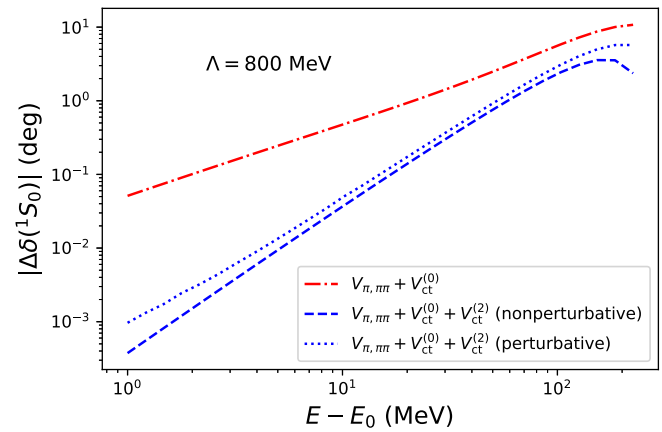

FIG. 7. Log-log plot of absolute differences to the reference phase shifts versus the energy difference to the matching point. The cutoff is 800 MeV. Results for the potentials $V_{\pi,\pi\pi} + V_{\rm ct}^{(0)}$ and $V_{\pi,\pi\pi} + V_{\rm ct}^{(0)} + V_{\rm ct}^{(2)}$ are shown as dash-dotted red and as blue lines, respectively. The dashed and the dotted blue line correspond to the nonperturbative and the perturbative inclusion of the subleading contact $V_{\rm ct}^{(2)}$, respectively.

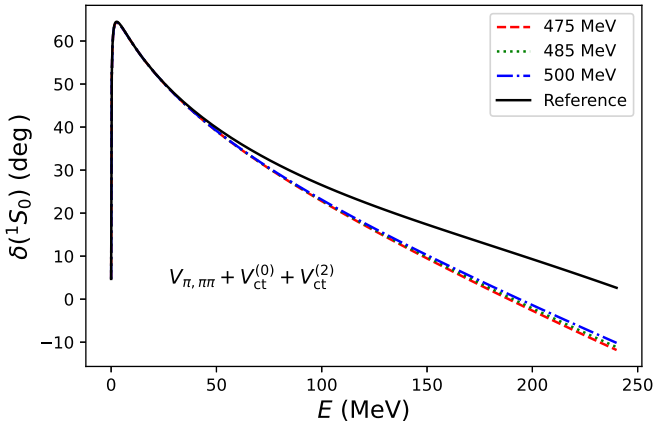

FIG. 8. The $^1S_0$ phase shifts as a function of the laboratory energy E with the interaction $V_{\pi,\pi\pi} + V_{ct}^{(0)} + V_{ct}^{(2)}$ at low cutoffs as indicated and compared to the reference (solid black line). The additional contact $V_{ct}^{(2)}$ restores the RG invariance that was lacking in Fig. 4.

Here, the subscript zero implies that all functions are evaluated at $(\tilde{C}_0, 0)$. We determine the derivatives numerically. Keeping the phase shift at E_0 unchanged implies

$$\left.\frac{\partial\delta(E_0)}{\partial\tilde{C}}\right|_0 \delta\tilde{C} + \left.\frac{\partial\delta(E_0)}{\partial C}\right|_0 \delta C = 0, \tag{13}$$

and, thus, a linear relation between $\delta\tilde{C}$ and δC. A one-parameter search along this line yields the optimal point that also reproduces the slope of the reference phase shifts at E_0. We can estimate this parameter by looking at

$$\delta(E) = \delta_0(E) + \alpha f_0(E), \tag{14}$$

with

$$f_0(E) \equiv \left(\frac{\partial\delta(E)}{\partial\tilde{C}}\frac{\partial\delta(E_0)}{\partial C} - \frac{\partial\delta(E)}{\partial C}\frac{\partial\delta(E_0)}{\partial\tilde{C}}\right)_0. \tag{15}$$

We seek the parameter α such that the phase shift be reproduced at the neighboring point E. Thus,

$$\alpha = \frac{\delta_{\rm Ref}(E) - \delta_0(E)}{f_0(E)}. \tag{16}$$

We then compute the resulting phase shifts using Eq. (12). The corresponding results are shown as blue dotted lines in Figs. 6 and 7. We see that the phase shifts from perturbative and nonperturbative solutions are close to each other, and that both yield a power-law improvement of our leading-order results. We also note that $\Lambda_b^2\delta C/(\tilde{C}_0 + \delta\tilde{C}) \approx -0.03$, and this is smaller in magnitude than expected from EFT estimates.

We also revisited the low cutoffs at and below the scale $\Lambda_{\rm TPE}$ in Eq. (11) and employed the subleading contact $V_{ct}^{(2)}$ in Eq. (8) nonperturbatively by matching the phase shift and its slope to the reference at a laboratory energy of 15 MeV. The results are shown in Fig. 8 and comparison with Fig. 4 shows that RG invariance is restored also at low momentum cutoffs.

Let us discuss other cutoffs. First, we checked whether the systematic improvements from the additional contact involving the LEC C discussed above are reproduced at larger cutoffs Λ while keeping $\Lambda_{\rm SFR}$ fixed at 700 MeV. Both perturbatively and nonperturbatively, we obtain improvements qualitatively identical to those shown in Fig. 7 for cutoff values up to $\Lambda \approx 2$ GeV. Second, we changed $\Lambda_{\rm SFR}$ to 900 MeV. In this case, we were able to obtain the same improvements, nonperturbatively, for cutoffs Λ as large as 4 GeV. Likewise, for $\Lambda_{\rm SFR} = 2$ GeV we also obtain the same power-law improvements up to $\Lambda = 4$ GeV in the nonperturbative approach. In the perturbative approach, however, fitting the additional contact to match the slope at E_0 at these larger values of $\Lambda_{\rm SFR}$ becomes numerically challenging for $\Lambda \gtrsim 1$ GeV.

IV. THE ROLE OF Δ ISOBAR DEGREES OF FREEDOM

The strong contributions of the subleading TPE in chiral EFT, i.e., the relatively large values of the pion-nucleon LECs c_i, are usually attributed to "resonance saturation." Consequently, these couplings become more natural in size when the Δ isobar degrees of freedom are included. Notably, such chiral EFTs have TPE terms that involve a Δ excitation already at NLO in the Weinberg power counting. The corresponding expressions for the potentials (2) were derived by Kaiser *et al.* [63] and we use those published by Krebs *et al.* [64] in their Eqs. (2.5)– (2.8). The chiral potential we employ thus consists of the OPE [given in Eq. (1)], leading TPE [given in Eqs. (3)], the contact (7), and the leading Δ contributions to TPE. In our numerical implementation this potential is regularized with $n = 4$ in the regulator (10) and spectral-function regularization was used with a cutoff of $\Lambda_{\rm SFR} = 700$ MeV.

We repeated the calculations presented above and found very similar results regarding the quality of the phase shifts in the $^1S_0$ partial wave, a breakdown momentum $\Lambda_b \approx$ 500 MeV, and a systematic power-law improvement when contact (8) quadratic in momenta is included. An example is shown in Fig. 9, to be compared with Fig. 6.

V. SUMMARY AND DISCUSSION

We analyzed chiral EFT in the $^1S_0$ partial wave and propose to promote the long-range parts of the leading and subleading TPE to accompany OPE along with a single contact $V_{ct}^{(0)}$ at leading order. Naturally, power counting in EFT applies to observables or amplitudes. Nevertheless, the promotion of the long-range parts of the TPE to leading order is inspired by the unexpectedly large matrix elements of the TPE potential that formally enter at NNLO in the Weinberg power counting. We find that our leading-order interaction cures two problems with the standard approach. First, the phase shifts in the $^1S_0$ partial wave are accurately reproduced and RG invariant for scattering energies of the order m_π^2/m_N and for large cutoffs. Second, the estimated breakdown momentum $\Lambda_b \approx 500$ MeV in $^1S_0$ is consistent with assumptions from chiral EFT. We also showed that adding a contact quadratic in momenta as a subleading correction leads to a systematic power-law improvement of the phase shifts. These results are based on an implementation of chiral EFT using spectral function regularization, and they are robust as the corresponding cutoff $\Lambda_{\rm SFR}$ is varied from 700to 900 MeV and to 2 GeV.

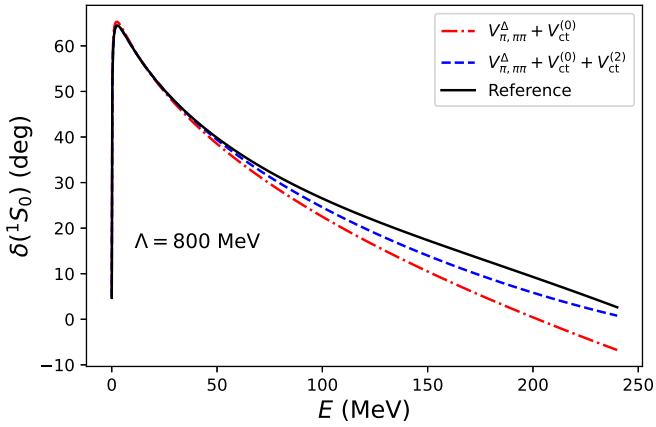

FIG. 9. The $^1S_0$ phase shifts as a function of the laboratory energy E for the $V^{\Delta}_{\pi,\pi\pi}$ interaction, i.e., our leading-order potential with Δ isobars included in the leading TPE potential. The dash-dotted red line uses a single contact $V^{(0)}_{\rm ct}$ to reproduce the value of the reference phase shift at $E_0 = 15$ MeV. The dashed blue line shows the phase shift when leading and subleading contacts $V^{(0)}_{\rm ct} + V^{(2)}_{\rm ct}$ are fit to reproduce the value and the slope of the reference phase shift at E_0. The cutoff is 800 MeV, and the reference phase shifts are shown as a solid black line. The results are close to those shown in Fig. 6.

We also pointed out that chiral EFTs with momentum cutoffs below about 500 MeV are really "two-pion-less" EFTs as they cut off parts of the TPE; in such cases higher-order contacts are needed for maintaining proper RG invariance. Lastly, we found that including the leading Δ contributions to TPE as a new leading-order contribution yields similar results.

We note that the proposed promotion of solely the long-range parts of TPE—while sufficient from an RG perspective—would preclude one to explore the quark-mass dependence of the resulting nucleon-nucleon potentials. Such studies need to include the polynomial terms of the TPE potential (see, e.g., Ref. [65]).

We also note that the chiral expansion of nucleon-nucleon forces converges only slowly (see Refs. [56,66]). This raises the question if higher orders of TPE should also be promoted. While we do not have a rigorous answer to this question, this work demonstrates that the proposed promotions are sufficient to address two known problems in the $^1S_0$ partial wave.

We finally remark that results shown in Fig. 1 seem to be consistent with model-independent large-N_c arguments from quantum chromodynamics [67–70]. In the limit of a large number of colors, N_c, potentials with the same spin/isospin structure as W_T, V_C, and W_S in Eq. (2) are leading order. We can easily identify the potential W_T with OPE, while V_C and W_S appear as contributions to subleading TPE. In contrast all potentials contributing to the leading TPE are suppressed by factors $1/N_c^2$ from large-N_c arguments. Figure 1 shows that the $^1S_0$ phase shifts are well described by a combination of OPE with subleading TPE while the impact of leading TPE is significantly smaller. Thus, promoting subleading TPE to one order before leading TPE could be seen as natural from the $1/N_c$ expansion. We therefore speculate that a combination of arguments from large N_c and chiral perturbation theory [71–76] could guide us in the construction of nuclear potentials.

ACKNOWLEDGMENTS

We thank Daniel Phillips for insightful and useful discussions. We also thank the participants of the INT program "Nuclear Forces for Precision Nuclear Physics (21-1b)" for many useful exchanges and discussions. This material is based upon work supported by the U.S. Department of Energy, Office of Science, Office of Nuclear Physics under Awards No. DE-FG02-96ER40963 and No. DE-SC0018223 (NUCLEI SciDAC-4 collaboration), and Contract No. DE-AC05-00OR22725 with UT-Battelle, LLC (Oak Ridge National Laboratory), the Swedish Research Council Grant No. 2020-005127, the European Research Council (ERC) under the European Union's Horizon 2020 research and innovation programme (Grant Agreement No. 758027), by the Deutsche Forschungsgemeinschaft (DFG, German Research Foundation) - Projektnummer 279384907 - CRC 1245, and by the National Science Foundation under Grants No. PHY-1555030 and No. PHY-2111426.

[1] H. Yukawa, On the interaction of elementary particles. I, Proc. Phys.-Math. Soc. Jpn. **17**, 48 (1935).
[2] S. Weinberg, Nuclear forces from chiral Lagrangians, Phys. Lett. B **251**, 288 (1990).
[3] S. Weinberg, Effective chiral Lagrangians for nucleon-pion interactions and nuclear forces, Nucl. Phys. B **363**, 3 (1991).
[4] C. Ordóñez and U. van Kolck, Chiral Lagrangians and nuclear forces, Phys. Lett. B **291**, 459 (1992).
[5] U. van Kolck, Few-nucleon forces from chiral Lagrangians, Phys. Rev. C **49**, 2932 (1994).
[6] N. Kaiser, R. Brockmann, and W. Weise, Peripheral nucleon-nucleon phase shifts and chiral symmetry, Nucl. Phys. A **625**, 758 (1997).
[7] E. Epelbaum, W. Glöckle, and U.-G. Meißner, Nuclear forces from chiral Lagrangians using the method of unitary transformation II: The two-nucleon system, Nucl. Phys. A **671**, 295 (2000).
[8] E. Epelbaum, H.-W. Hammer, and U.-G. Meißner, Modern theory of nuclear forces, Rev. Mod. Phys. **81**, 1773 (2009).
[9] H. W. Hammer, S. König, and U. van Kolck, Nuclear effective field theory: Status and perspectives, Rev. Mod. Phys. **92**, 025004 (2020).
[10] J. A. Melendez, S. Wesolowski, and R. J. Furnstahl, Bayesian truncation errors in chiral effective field theory: Nucleon-nucleon observables, Phys. Rev. C **96**, 024003 (2017).
[11] P. Reinert, H. Krebs, and E. Epelbaum, Semilocal momentum-space regularized chiral two-nucleon potentials up to fifth order, Eur. Phys. J. A **54**, 86 (2018).
[12] S. Wesolowski, R. J. Furnstahl, J. A. Melendez, and D. R. Phillips, Exploring Bayesian parameter estimation for chiral effective field theory using nucleon-nucleon phase shifts, J. Phys. G: Nucl. Part. Phys. **46**, 045102 (2019).
[13] R. J. Furnstahl, H. W. Hammer, and A. Schwenk, Nuclear structure at the crossroads, Few-Body Syst. **62**, 72 (2021).

[14] P. Maris, E. Epelbaum, R. J. Furnstahl, J. Golak, K. Hebeler, T. Hüther, H. Kamada, H. Krebs, U.-G. Meißner, J. A. Melendez, A. Nogga, P. Reinert, R. Roth, R. Skibiński, V. Soloviov, K. Topolnicki, J. P. Vary, Y. Volkotrub, H. Witała, and T. Wolfgruber (LENPIC Collaboration), Light nuclei with semilocal momentum-space regularized chiral interactions up to third order, Phys. Rev. C **103**, 054001 (2021).

[15] C.-J. Yang, A. Ekström, C. Forssén, and G. Hagen, Power counting in chiral effective field theory and nuclear binding, Phys. Rev. C **103**, 054304 (2021).

[16] D. B. Kaplan, M. J. Savage, and M. B. Wise, Nucl. Phys. B **478**, 629 (1996).

[17] D. B. Kaplan, M. J. Savage, and M. B. Wise, A new expansion for nucleon-nucleon interactions, Phys. Lett. B **424**, 390 (1998).

[18] T. Frederico, V. S. Timoteo, and L. Tomio, Renormalization of the one pion exchange interaction, Nucl. Phys. A **653**, 209 (1999).

[19] A. Nogga, R. G. E. Timmermans, and U. van Kolck, Renormalization of one-pion exchange and power counting, Phys. Rev. C **72**, 054006 (2005).

[20] M. Pavón. Valderrama and E. R. Arriola, Renormalization of the deuteron with one pion exchange, Phys. Rev. C **72**, 054002 (2005).

[21] M. Pavón Valderrama and E. Ruiz Arriola, Renormalization of the *NN* interaction with a chiral two-pion-exchange potential: Central phases and the deuteron, Phys. Rev. C **74**, 054001 (2006).

[22] M. C. Birse, Power counting with one-pion exchange, Phys. Rev. C **74**, 014003 (2006).

[23] D. Shukla, D. R. Phillips, and E. Mortenson, Chiral potentials, perturbation theory and the $^1S_0$ channel of NN scattering, J. Phys. G: Nucl. Part. Phys. **35**, 115009 (2008).

[24] C.-J. Yang, C. Elster, and D. R. Phillips, Subtractive renormalization of the *NN* scattering amplitude at leading order in chiral effective theory, Phys. Rev. C **77**, 014002 (2008).

[25] M. C. Birse, Deconstructing $^1S_0$ nucleon-nucleon scattering, Eur. Phys. J. A **46**, 231 (2010).

[26] B. Long and C.-J. Yang, Short-range nuclear forces in singlet channels, Phys. Rev. C **86**, 024001 (2012).

[27] B. Long and C.-J. Yang, Renormalizing chiral nuclear forces: Triplet channels, Phys. Rev. C **85**, 034002 (2012).

[28] M. Pavón. Valderrama and D. R. Phillips, Power Counting of Contact-Range Currents in Effective Field Theory, Phys. Rev. Lett. **114**, 082502 (2015).

[29] M. S. Sánchez, C.-J. Yang, B. Long, and U. van Kolck, Two-nucleon $^1S_0$ amplitude zero in chiral effective field theory, Phys. Rev. C **97**, 024001 (2018).

[30] D. Odell, A. Deltuva, J. Bonilla, and L. Platter, Renormalization of a finite-range inverse-cube potential, Phys. Rev. C **100**, 054001 (2019).

[31] M. Sánchez Sánchez, N. A. Smirnova, A. M. Shirokov, P. Maris, and J. P. Vary, Improved description of light nuclei through chiral effective field theory at leading order, Phys. Rev. C **102**, 024324 (2020).

[32] U. van Kolck, The problem of renormalization of chiral nuclear forces, Front. Phys. **8**, 79 (2020).

[33] D. R. Entem and R. Machleidt, Accurate charge-dependent nucleon-nucleon potential at fourth order of chiral perturbation theory, Phys. Rev. C **68**, 041001(R) (2003).

[34] G. P. Lepage, How to renormalize the Schrodinger equation, arXiv:nucl-th/9706029.

[35] M. Pavón Valderrama, Perturbative renormalizability of chiral two-pion exchange in nucleon-nucleon scattering, Phys. Rev. C **83**, 024003 (2011).

[36] E. Epelbaum, A. M. Gasparyan, J. Gegelia, and H. Krebs, $^1S_0$ nucleon-nucleon scattering in the modified Weinberg approach, Eur. Phys. J. A **51**, 71 (2015).

[37] M. Pavón Valderrama, Perturbative renormalizability of chiral two pion exchange and power counting in nucleon-nucleon scattering, in *International Workshop on Chiral Symmetry in Hadrons and Nuclei*, edited by J. M. Nieves, E. Oset, and M. J. Vicente-Vacas, AIP Conf. Proc. No. 1322 (AIP, New York, 2010), p. 205.

[38] M. Pavón Valderrama, Scattering amplitudes versus potentials in nuclear effective field theory: Is there a potential compromise? arXiv:1902.08172.

[39] M. Pavón Valderrama, A comparison of two possible nuclear effective field theory expansions around the one- and two-pion exchange potentials, arXiv:2112.02076.

[40] W. Frank, D. J. Land, and R. M. Spector, Singular potentials, Rev. Mod. Phys. **43**, 36 (1971).

[41] R. B. Wiringa, V. G. J. Stoks, and R. Schiavilla, Accurate nucleon-nucleon potential with charge-independence breaking, Phys. Rev. C **51**, 38 (1995).

[42] R. Machleidt, High-precision, charge-dependent Bonn nucleon-nucleon potential, Phys. Rev. C **63**, 024001 (2001).

[43] J. R. Peláez, From controversy to precision on the sigma meson: A review on the status of the non-ordinary f0 (500) resonance, Phys. Rep. **658**, 1 (2016).

[44] I. Caprini, G. Colangelo, and H. Leutwyler, Mass and Width of the Lowest Resonance in QCD, Phys. Rev. Lett. **96**, 132001 (2006).

[45] J. D. Walecka, The relativistic nuclear many-body problem, in *New Vistas in Nuclear Dynamics*, NATO ASI Series (Series B: Physics), Vol. 139, edited by P. J. Brussaard and J. H. Koch (Springer, Boston, 1986), pp. 229–271.

[46] P.-G. Reinhard, The relativistic mean-field description of nuclei and nuclear dynamics, Rep. Prog. Phys. **52**, 439 (1989).

[47] Y. K. Gambhir, P. Ring, and A. Thimet, Relativistic mean field theory for finite nuclei, Ann. Phys. **198**, 132 (1990).

[48] B. D. Serot and J. D. Walecka, Relativistic nuclear many-body theory, in *Recent Progress in Many-Body Theories*, edited by T. L. Ainsworth, C. E. Campbell, B. E. Clements, and E. Krotscheck (Springer, Boston, 1992), pp. 49–92.

[49] Y. Sugahara and H. Toki, Relativistic mean-field theory for unstable nuclei with non-linear σ and ω terms, Nucl. Phys. A **579**, 557 (1994).

[50] J. F. Donoghue, Sigma exchange in the nuclear force and effective field theory, Phys. Lett. B **643**, 165 (2006).

[51] R. J. Crewther and L. C. Tunstall, $\Delta I = 1/2$ rule for kaon decays derived from QCD infrared fixed point, Phys. Rev. D **91**, 034016 (2015).

[52] Y.-L. Ma and M. Rho, Towards the hadron-quark continuity via a topology change in compact stars, Prog. Part. Nucl. Phys. **113**, 103791 (2020).

[53] R. Machleidt and D. Entem, Chiral effective field theory and nuclear forces, Phys. Rep. **503**, 1 (2011).

[54] A. Ekström, G. Baardsen, C. Forssén, G. Hagen, M. Hjorth-Jensen, G. R. Jansen, R. Machleidt, W. Nazarewicz, T. Papenbrock, J. Sarich, and S. M. Wild, Optimized Chiral Nucleon-Nucleon Interaction at Next-to-Next-to-Leading Order, Phys. Rev. Lett. **110**, 192502 (2013).

[55] A. Ekström, G. R. Jansen, K. A. Wendt, G. Hagen, T. Papenbrock, B. D. Carlsson, C. Forssén, M. Hjorth-Jensen, P. Navrátil, and W. Nazarewicz, Accurate nuclear radii and binding energies from a chiral interaction, Phys. Rev. C **91**, 051301(R) (2015).

[56] D. R. Entem, N. Kaiser, R. Machleidt, and Y. Nosyk, Peripheral nucleon-nucleon scattering at fifth order of chiral perturbation theory, Phys. Rev. C **91**, 014002 (2015).

[57] W. G. Jiang, A. Ekström, C. Forssén, G. Hagen, G. R. Jansen, and T. Papenbrock, Accurate bulk properties of nuclei from $a = 2$ to ∞ from potentials with Δ isobars, Phys. Rev. C **102**, 054301 (2020).

[58] M. Hoferichter, J. Ruiz de Elvira, B. Kubis, and U.-G. Meißner, Matching Pion-Nucleon Roy-Steiner Equations to Chiral Perturbation Theory, Phys. Rev. Lett. **115**, 192301 (2015).

[59] M. Hoferichter, J. Ruiz de Elvira, B. Kubis, and U.-G. Meißner, Roy-Steiner-equation analysis of pion-nucleon scattering, Phys. Rep. **625**, 1 (2016).

[60] E. Epelbaum, W. Gloeckle, and U.-G. Meissner, Improving the convergence of the chiral expansion for nuclear forces. 1. Peripheral phases, Eur. Phys. J. A **19**, 125 (2004).

[61] E. Epelbaum, W. Glöckle, and U.-G. Meißner, Improving the convergence of the chiral expansion for nuclear forces - II: Low phases and the deuteron, Eur. Phys. J. A **19**, 401 (2004).

[62] R. N. Pérez, J. E. Amaro, and E. R. Arriola, Coarse-grained potential analysis of neutron-proton and proton-proton scattering below the pion production threshold, Phys. Rev. C **88**, 064002 (2013).

[63] N. Kaiser, S. Gerstendörfer, and W. Weise, Peripheral NN-scattering: Role of delta-excitation, correlated two-pion and vector meson exchange, Nucl. Phys. A **637**, 395 (1998).

[64] H. Krebs, E. Epelbaum, and U. G. Meißner, Nuclear forces with Δ excitations up to next-to-next-to-leading order, part I: Peripheral nucleon-nucleon waves, Eur. Phys. J. A **32**, 127 (2007).

[65] E. Epelbaum, U.-G. Meißner, and W. Glöckle, Nuclear forces in the chiral limit, Nucl. Phys. A **714**, 535 (2003).

[66] D. R. Entem, N. Kaiser, R. Machleidt, and Y. Nosyk, Dominant contributions to the nucleon-nucleon interaction at sixth order of chiral perturbation theory, Phys. Rev. C **92**, 064001 (2015).

[67] D. B. Kaplan and A. V. Manohar, Nucleon-nucleon potential in the $1/N_c$ expansion, Phys. Rev. C **56**, 76 (1997).

[68] M. K. Banerjee, T. D. Cohen, and B. A. Gelman, Nucleon-nucleon interaction and large N_c QCD, Phys. Rev. C **65**, 034011 (2002).

[69] T. D. Cohen, Resolving the large-N_c nuclear potential puzzle, Phys. Rev. C **66**, 064003 (2002).

[70] M. M. Kaskulov and H. Clement, Correlated two-pion exchange and large-N_c behavior of nuclear forces, Phys. Rev. C **70**, 014002 (2004).

[71] M. A. Luty, J. March-Russell, and M. White, Baryon magnetic moments in a simultaneous expansion in $1/n$ and m_s, Phys. Rev. D **51**, 2332 (1995).

[72] E. Jenkins, Chiral Lagrangian for baryons in the $\frac{1}{N_c}$ expansion, Phys. Rev. D **53**, 2625 (1996).

[73] R. Flores-Mendieta, Baryon magnetic moments in large-N_c chiral perturbation theory, Phys. Rev. D **80**, 094014 (2009).

[74] G. Ahuatzin, R. Flores-Mendieta, M. A. Hernández-Ruiz, and C. P. Hofmann, Baryon magnetic moments in large-N_c chiral perturbation theory: Effects of the decuplet-octet mass difference and flavor symmetry breaking, Phys. Rev. D **89**, 034012 (2014).

[75] I. P. Fernando and J. L. Goity, Baryon chiral perturbation theory combined with the $1/\mathrm{N_c}$ expansion in SU(3): Framework, Phys. Rev. D **97**, 054010 (2018).

[76] D. Lee *et al.*, Hidden Spin-Isospin Exchange Symmetry, Phys. Rev. Lett. **127**, 062501 (2021).